Performance Analysis of Up-link and Down-link Mixed RF/FSO Links with Multiple Relays

Chadi Abou-Rjeily, *Member IEEE*
Department of Electrical and Computer Engineering
Lebanese American University (LAU), Byblos, Lebanon
chadi.abourjeily@lau.edu.lb

***Abstract*—This paper targets the bit error rate (BER) performance analysis of mixed radio-frequency free-space optical (RF/FSO) communication systems with a single source, single destination and multiple relays operating in the decode-and-forward (DF) mode. Several relaying scenarios are analyzed and compared for both the up-link (RF hop followed by an FSO hop) and the down-link (FSO hop followed by an RF hop). The RF links are subject to Nakagami fading and corrupted by additive Gaussian noise while the FSO links are subject to gamma-gamma scintillation where the photons generated by the background noise and dark currents follow the Poisson distribution.**

***Index Terms*—Free Space Optics, Radio Frequency, RF, Relaying, BER, Atmospheric Turbulence, Nakagami, Gamma-Gamma.**

I. Introduction

Free-space optical (FSO) communications are attracting a significant attention as a high-speed low-cost solution for solving the last mile problem. Despite the numerous advantages of FSO communications, these systems suffer from the two following main limitations. Since FSO is based on optical communications, establishing an FSO link necessitates the presence of a direct line-of-sight (LOS) between the communicating nodes. Consequently, FSO networks can not support mobility and the FSO connections can not be established for any network setup following from the imposed geographic constraints. On the other hand, severe weather conditions, like fog or snow, result in very large attenuation values rendering the FSO links almost useless under such weather conditions [1]. These limitations motivated the analysis of hybrid RF/FSO systems as well as mixed RF/FSO communications.

In hybrid RF/FSO systems, an RF link is used as a backup for the FSO link [2]–[4]. For such systems, the high-speed FSO link is activated when the atmospheric weather conditions are favorable; otherwise, the transceivers will switch to the lower-speed but more reliable RF links. Both hard switching [2] and soft switching [3], [4] were envisaged in the literature where, in the first case, only one of the two available RF or FSO links is activated while, in the second case, encoding/decoding are jointly performed over both links for an enhanced system performance. On the other hand, for mixed RF/FSO systems, the RF and FSO links are cascaded in series [5]–[9]. Such systems correspond typically to dual-hop relaying systems where one hop is RF while the second hop is FSO. The outage probability for a single-user single-relay mixed RF/FSO scheme was derived in [5] with amplify-and-forward (AF) relaying. Multiuser single-relay decode-and-forward (DF) mixed RF/FSO systems were analyzed in [6], [7] where the relay is equipped with multiple antenna for separating the signals received from the mobile users. While [6] considered the ordered successive interference cancelation, [7] tackled the problem of link allocation with delay-limited and delay-tolerant designs. While [5]–[7] considered the case of a single relay, multiple AF relays were considered in the study that has been carried out in [8]. Finally, while in [5]–[8] the first single-user or multiuser hop was RF and the second hop was FSO, [9] considered the case of an FSO hop followed by an RF hop where AF relaying was considered with a single relay that serves a number of RF users.

This paper targets the performance analysis of mixed RF/FSO systems in the presence of N AF relays. Unlike [5]–[7], [9], we consider the case of multiple relays. Moreover, unlike [5], [8], [9] that are based on AF relaying, we consider the case of DF relaying. Finally, unlike all previous contributions where the additive white Gaussian noise (AWGN) model was adopted for the FSO links [5]–[9], we consider a more realistic noise model where the number of photoelectrons generated by noise follows the Poisson distribution. Unlike the AWGN model that holds for shot noise limited receivers [10], the adopted Poisson model can be applied with no assumptions on the receiver. The presence of two types of noises clearly distinguishes the presented performance analysis from the existing studies in the literature. Moreover, the presence of multiple relays offers a number of option in what concerns the design of the relaying protocol. In this context, we analyze and compare three relaying protocols for the up-link system (RF-FSO) and two schemes for the down-link system (FSO-RF). These protocols have different channel state information (CSI) and symbol selectivity (SS) requirements and they allow to achieve different levels of compromise between complexity and performance as will be highlighted later.

II. System Model

Consider a mixed RF/FSO communication system with N relays as depicted in Fig. 1. The communication between the source node (S) and the destination node (D) takes place in a dual-hop manner by making use of the presence of the N relays denoted by $\mathrm{R}_1, \ldots, \mathrm{R}_N$ where we assume that no direct link is available between S and D. The relays are assumed to operate in the Decode-and-Forward (DF) manner. In other

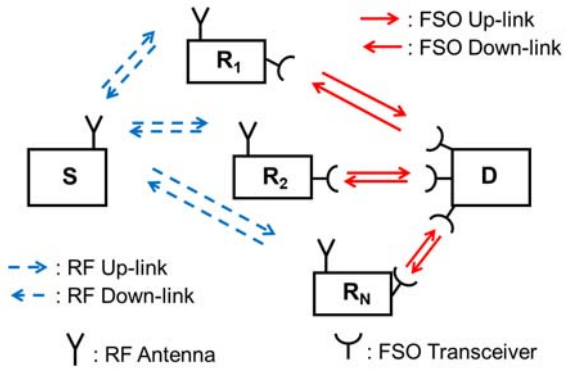

Fig. 1. The analyzed mixed RF/FSO communication system in the up-link and the down-link.

words, the received messages are decoded at the relays prior to their potential retransmission to the destination node. In the up-link, the communications take place from S to D. In the first hop, S broadcasts the information message to the N relays along the RF link while, in the second hop, the relays retransmit the decoded messages to D along the N FSO links. On the other hand, in the down-link, communications take place from D to S. In this case, the first hop involves FSO communications while the second hop involved RF transmissions. Several relaying protocols will be discussed and analyzed in each one of the above scenarios.

In what follows, we highlight the basic parameters of each one of the RF and FSO links.

A. RF Links

The equivalent output-input relation along the RF link S-R$_n$ is given by:

$$x_n = \sqrt{k_n E_b} h_n s + w_n \tag{1}$$

where x_n and s stand for the received and transmitted signals, respectively. In (1), w_n stands for the additive white Gaussian noise (AWGN) at the n-th relay where this noise term is assumed to have a zero mean with variance $N_0/2$. In what follows, we assume that binary phase shift keying (BPSK) is used along the RF links and the bit energy is denoted by E_b.

In (1), h_n stands for the path gain along the RF link S-R$_n$. In this work, we consider the Nakagami fading model where h_n is assumed to follow the Nakagami distribution with parameter m_n whose probability density function (pdf) is given by:

$$f_n^{(\text{Nak})}(h) = 2\frac{(m_n/\Omega_n)^{m_n}}{\Gamma(m_n)} h^{2m_n-1} \exp\left(-\frac{m_n h^2}{\Omega_n}\right) \;\; ; \;\; h \geq 0 \tag{2}$$

where $m_n > 0.5$ is the shaping parameter, Ω_n is the mean power and $\Gamma(.)$ stands for the Gamma function.

Finally, the constant k_n is introduced in (1) to take into account the fact that the relays might not be at the same distance from S. Considering the S-D link as the reference link and assuming a square-law power attenuation along the RF links, k_n takes the following value:

$$k_n = \left(\frac{d_{0,N+1}}{d_{0,n}}\right)^2 \tag{3}$$

where $d_{0,N+1}$ stands for the distance between S (also referred to as R$_0$) and D (also referred to as R$_{N+1}$) while $d_{0,n}$ stands for the distance between S and R$_n$.

Following from the reciprocity of the RF channel, the system model in (1) holds for the communications between R$_n$ and S in the down-link as well.

B. FSO Links

We assume that the FSO links are subject to gamma-gamma turbulence-induced fading. In this case, the pdf of the channel irradiance I_n along the FSO link R$_n$-D is given by:

$$f_n^{(\gamma\gamma)}(I) = \frac{2(\alpha_n\beta_n)^{(\alpha_n+\beta_n)/2}}{\Gamma(\alpha_n)\Gamma(\beta_n)} I^{(\alpha_n+\beta_n)/2-1} K_{\alpha_n-\beta_n}\left(2\sqrt{\alpha_n\beta_n I}\right) \;\; ; \;\; I \geq 0 \tag{4}$$

where $K_c(.)$ is the modified Bessel function of the second kind of order c. The parameters α_n and β_n are given by:

$$\alpha_n = \left[\exp\left(\frac{0.49\sigma_R^2(d_{n,N+1})}{(1+1.11\sigma_R^{12/5}(d_{n,N+1}))^{7/6}}\right) - 1\right]^{-1} \tag{5}$$

$$\beta_n = \left[\exp\left(\frac{0.51\sigma_R^2(d_{n,N+1})}{(1+0.69\sigma_R^{12/5}(d_{n,N+1}))^{5/6}}\right) - 1\right]^{-1} \tag{6}$$

where $\sigma_R^2(d)$ is the Rytov variance related to the link distance d by $\sigma_R^2(d) = 1.23C_n^2k^{7/6}d^{11/6}$ where k is the wave number and C_n^2 denotes the refractive index structure parameter.

Binary Pulse Position Modulation (PPM) is applied with Intensity-Modulation and Direct-Detection (IM/DD) along the FSO links. In this case, the bit duration T_b is divided into two time slots and an optical signal is transmitted in only one of these slots. The receiver consists of a photo-counter that counts the number of photoelectrons generated in each slot and decides in favor of the slot having the maximum count. In this case, the average numbers of photoelectrons generated in the "on" and "off" slots are given by [11]:

$$\text{E}[X_n^{(\text{on})}] = p_n g_n I_n \lambda_s + \lambda_b \;\; ; \;\; \text{E}[X_n^{(\text{off})}] = \lambda_b \tag{7}$$

where E[.] stands for the averaging operator and I_n is the channel irradiance whose pdf is given in (4) and that satisfies E$[I_n] = 1$. In (7), λ_s and λ_b stand for the average numbers of photoelectrons generated by the incident light signal (in the absence of channel scintillation) and by the background radiation (and dark currents), respectively:

$$\lambda_s = \eta\frac{P_s T_b/2}{hf} \triangleq \eta\frac{E_s}{hf} \;\; ; \;\; \lambda_b = \eta\frac{P_b T_b/2}{hf} \tag{8}$$

where P_s and P_b stand for the incident optical power and the power of background noise, respectively. T_b stands for the bit duration, η is the detector's quantum efficiency assumed to be equal to 0.5, h is Planck's constant and f is the optical center

frequency taken to be 1.94×10^{14} Hz (corresponding to a wavelength of 1550 nm). Finally, $E_s = P_s T_b/2$ corresponds to the received optical energy per PPM slot.

In (7), p_n stands for the fraction of the total optical power that is allocated to the n-th FSO link with $0 \leq p_n \leq 1$ and $\sum_{n=1}^{N} p_n = 1$. Finally, in a way similar to (3), g_n is a gain factor associated with the link R_n-D that might be shorter than the direct link S-D. In this context [10]:

$$g_n = \left(\frac{d_{0,N+1}}{d_{n,N+1}}\right)^2 e^{-\sigma(d_{n,N+1}-d_{0,N+1})} \tag{9}$$

where σ is the attenuation coefficient.

Finally, following from the reciprocity of the FSO links, the FSO system model presented in this subsection holds for the communications between D and R_n in the down-link.

III. Performance Analysis

A. Performance Analysis along the Up-Link

Several relaying strategies can be envisaged for the dual-hop up-link communications. While in the first RF hop, the unique option is for S to broadcast the information symbol s that will be eventually overheard by all relays, the numerous strategies arise from the different roles that can be played by the relays and by the different ways in which these relays opt to activate the FSO links. For the FSO link, symbol selectivity (SS) can be applied or not. SS refers to the option that the relay forwards the decoded message to D only in the case where this symbol has been decoded correctly. In this case, a channel code along with a parity check operation can be implemented so that the relay R_n can decide on whether the decision it made on s was correct or not. In the first case, s will be forwarded to D along the FSO link R_n-D; otherwise, no message will be forwarded from R_n to D. Intuitively, SS results in a better performance at the expense of an increased complexity for performing the cyclic redundancy check.

The second parameter that dictates the relaying strategy is whether the channel state information (CSI) is available or not. In the absence of CSI, the values of the N FSO channel gains $I_1, \ldots, I_N$ are not acquired and, in this case, all relays participate in the cooperation effort regardless of the state of the corresponding relay-destination FSO link. For this scenario, no relay is given preference over the others and $p_1 = \cdots = p_N = \frac{1}{N}$ in (7). In the presence of CSI, only the best relay-destination link is activated resulting in $p_{\hat{n}} = 1$ and $p_n = 0$ for $n \neq \hat{n}$ where $\hat{n} \triangleq \arg\max\{g_n I_n\}$ where $\hat{n}$ stands for the index of the selected relay-destination FSO link. Evidently, the selection has to be made between the relays that have successfully decoded the message; otherwise, the wrong replica of the message will be forwarded to D enforcing a decision that will be erroneous with a very high probability. Evidently, acquiring the CSI increases the system complexity where training symbols must be exchanged between the different communicating nodes for the sake of estimating the channel; however, this acquisition will result in enhanced performance levels. In this case, the large coherence time of the FSO channels (that is in the order of msec) facilitates the channel estimation task since acquiring the values of the FSO path gains does not need to be carried out very often. On the other hand, acquiring the CSI defeats the purpose of noncoherent IM/DD communications that can be implemented in a very simple and cost-effective manner.

In what follows, three relaying protocols will be discussed, analyzed and compared based on the implementation of SS and availability of CSI. As indicated above, these protocols differ only by the way communications are carried out along the second FSO hop. From (1), the conditional bit error rate (BER) along the RF link S-R_n is given by $Q\left(\sqrt{\frac{2k_n E_b}{N_0}} h_n\right)$ where $Q(x) = \frac{1}{\sqrt{2\pi}} \int_x^\infty e^{-\frac{t^2}{2}} \mathrm{d}t$ stands for the Q-function.

1) NSS-NCSI Scheme: The first protocol can be implemented with no symbol selectivity (NSS) in the absence of CSI (NCSI).

Consider a subset $\mathcal{S}$ of $\{1, \ldots, N\}$ and assume that the relays R_n for $n \in \mathcal{S}$ have successfully decoded the information symbol s. In this case, these relays will be transmitting light signals in the correct PPM slot along the second FSO hop while the remaining relays in $\overline{\mathcal{S}} \triangleq \{1, \ldots, N\} \backslash \mathcal{S}$ will be transmitting light signals in the second (i.e. erroneous) PPM slot. Consequently, for equal gain combining (EGC) at the receiver, the average number of photoelectrons in the "on" and "off" slots can be written as:

$$\mathrm{E}[X^{(\mathrm{on})}_{\text{NSS-NCSI}}] = \left(\frac{1}{N} \sum_{n \in \mathcal{S}} g_n I_n\right) \lambda_s + N\lambda_b \tag{10}$$

$$\mathrm{E}[X^{(\mathrm{off})}_{\text{NSS-NCSI}}] = \left(\frac{1}{N} \sum_{n \in \overline{\mathcal{S}}} g_n I_n\right) \lambda_s + N\lambda_b \tag{11}$$

where λ_b was multiplied by N because of the noise accumulation at the receiver following from EGC. Finally, for NCSI, the power is evenly split among all N links justifying the normalizing factor $1/N$ (multiplying the term λ_s).

Denote by X_1 the Poisson random variable (rv) whose parameter is $\mathrm{E}[X^{(\mathrm{on})}_{\text{NSS-NCSI}}]$ and by X_2 the Poisson rv whose parameter is $\mathrm{E}[X^{(\mathrm{off})}_{\text{NSS-NCSI}}]$. The conditional probability of error at D can be calculated from $\Pr(X_2 > X_1) + \frac{1}{2}\Pr(X_2 = X_1)$ where, in the first case, the photon-counter will decide in favor of the wrong "off" slot while, in the second case, the random tie breaking between the two PPM slots results in an erroneous decision with probability $1/2$. Developing this expression and taking into consideration the error probabilities along the RF source-relay links, the conditional BER of the NSS-NCSI scheme can be developed as shown in (12) at the top of the next page. In (12), the notation $\sum_{\mathcal{S} \subset \{1,\ldots,N\}}$ denotes that the summation is carried out over all possible subsets $\mathcal{S}$ of $\{1, \ldots, N\}$. This BER is conditioned over the N RF channels $\mathcal{H} \triangleq \{h_n\}_{n=1}^N$ and over the N FSO channels $\mathcal{I} \triangleq \{I_n\}_{n=1}^N$.

2) SS-NCSI Scheme: When symbol selectivity is applied on the symbols to be forwarded from the relays, transmission in the wrong PPM slot are refrained. Consequently, while the average number of photoelectrons in the "on" slot in (10) keeps the same expression, the signal term comprised in the average

$$P_{e|\mathcal{H},\mathcal{I}}^{(\text{NSS-NCSI})} = \sum_{\mathcal{S}\subset\{1,\ldots,N\}} \prod_{n\in\mathcal{S}} \left(1 - Q\left(\sqrt{\frac{2k_nE_b}{N_0}}h_n\right)\right) \prod_{n'\in\overline{\mathcal{S}}} Q\left(\sqrt{\frac{2k_{n'}E_b}{N_0}}h_{n'}\right)$$
$$\left[\sum_{k=0}^{+\infty} e^{-\left(\left(\frac{1}{N}\sum_{n\in\overline{\mathcal{S}}} g_nI_n\right)\lambda_s+N\lambda_b\right)} \frac{\left(\left(\frac{1}{N}\sum_{n\in\overline{\mathcal{S}}} g_nI_n\right)\lambda_s+N\lambda_b\right)^k}{k!} \sum_{j=0}^{k-1} e^{-\left(\left(\frac{1}{N}\sum_{n\in\mathcal{S}} g_nI_n\right)\lambda_s+N\lambda_b\right)} \frac{\left(\left(\frac{1}{N}\sum_{n\in\mathcal{S}} g_nI_n\right)\lambda_s+N\lambda_b\right)^j}{j!}\right.$$
$$\left.+\frac{1}{2}\sum_{k=0}^{+\infty} e^{-\left(\left(\frac{1}{N}\sum_{n\in\overline{\mathcal{S}}} g_nI_n\right)\lambda_s+N\lambda_b\right)} \frac{\left(\left(\frac{1}{N}\sum_{n\in\overline{\mathcal{S}}} g_nI_n\right)\lambda_s+N\lambda_b\right)^k}{k!} e^{-\left(\left(\frac{1}{N}\sum_{n\in\mathcal{S}} g_nI_n\right)\lambda_s+N\lambda_b\right)} \frac{\left(\left(\frac{1}{N}\sum_{n\in\mathcal{S}} g_nI_n\right)\lambda_s+N\lambda_b\right)^k}{k!}\right] \quad (12)$$

number of photoelectrons in the "off" slot in (11) needs to be removed. In other words, (10) and (11) will be written as:

$$\mathrm{E}[X_{\text{SS-NCSI}}^{(\text{on})}] = \left(\frac{1}{N}\sum_{n\in\mathcal{S}} g_nI_n\right)\lambda_s + N\lambda_b \quad (13)$$

$$\mathrm{E}[X_{\text{SS-NCSI}}^{(\text{off})}] = N\lambda_b \quad (14)$$

Following the same calculation procedures as in the case of NSS-NCSI, the conditional BER of the SS-NCSI scheme can be written as shown in (15) on the top of the next page.

3) SS-CSI Scheme: In the presence of CSI and when symbol selectivity is applied, transmissions occur only along the strongest relay-destination FSO link with full optical power. In this case, the average numbers of photoelectrons in (13)-(14) will take the following expressions:

$$\mathrm{E}[X_{\text{SS-CSI}}^{(\text{on})}] = \max_{n\in\mathcal{S}}\{g_nI_n\}\lambda_s + N\lambda_b \quad (16)$$

$$\mathrm{E}[X_{\text{SS-CSI}}^{(\text{off})}] = N\lambda_b \quad (17)$$

Therefore, the conditional BER of the SS-CSI scheme can be written as shown in (18) on the top of the next page.

4) Average BER and comparing the different schemes: The average BER can be obtained by averaging the conditional BER over the N RF path gains and the N FSO path gains:

$$P_e = \underbrace{\int_0^{+\infty}\cdots\int_0^{+\infty}}_{2N \text{ times}} P_{e|\mathcal{H},\mathcal{I}} \prod_{n=1}^{N} [f_n^{(\text{Nak})}(h_n) f_n^{(\gamma\gamma)}(I_n)] \, \mathrm{d}h_1\cdots\mathrm{d}h_N\mathrm{d}I_1\cdots\mathrm{d}I_N \quad (19)$$

where $P_{e|\mathcal{H},\mathcal{I}}$ stands for any one of the conditional BERs $P_{e|\mathcal{H},\mathcal{I}}^{(\text{NSS-NCSI})}$, $P_{e|\mathcal{H},\mathcal{I}}^{(\text{SS-NCSI})}$ and $P_{e|\mathcal{H},\mathcal{I}}^{(\text{SS-CSI})}$ given in (12), (15) and (18), respectively. Given the complexity of these conditional BER expressions, it is very hard to solve the $2N$ integrals in (19) in an analytical manner. These integrals can be solved by numerically integrating over the pdf's of the path gains.

From (10), (13) and (16), it can be observed that:

$$\mathrm{E}[X_{\text{SS-CSI}}^{(\text{on})}] \geq \mathrm{E}[X_{\text{SS-NCSI}}^{(\text{on})}] = \mathrm{E}[X_{\text{NSS-NCSI}}^{(\text{on})}] \quad (20)$$

Similarly, comparing (11), (14) and (17), it can be observed that:

$$\mathrm{E}[X_{\text{SS-CSI}}^{(\text{off})}] = \mathrm{E}[X_{\text{SS-NCSI}}^{(\text{of})}] \leq \mathrm{E}[X_{\text{NSS-NCSI}}^{(\text{off})}] \quad (21)$$

where the comparisons in (20) and (21) hold for all possible values of the sets $\mathcal{S}$, $\mathcal{H}$ and $\mathcal{I}$.

In other words, while moving from the NSS-NCSI scheme to the SS-NCSI scheme to the SS-CSI scheme, the average number of photoelectrons in the correct slot is increasing while the average number of photoelectrons in the wrong slot is decreasing thus contributing to decreasing the value of the BER (note that the first two multiplicative terms in (12), (15) and (18) are the same). As a conclusion:

$$P_{e|\mathcal{H},\mathcal{I}}^{(\text{SS-CSI})} \leq P_{e|\mathcal{H},\mathcal{I}}^{(\text{SS-NCSI})} \leq P_{e|\mathcal{H},\mathcal{I}}^{(\text{NSS-NCSI})} \quad (22)$$

where this comparison holds for any network scenario. This highlights the positive impact of the symbol selectivity and CSI acquisition on enhancing the system performance.

B. Performance Analysis along the Down-Link

For the down-link communications, two relaying schemes can be implemented depending on the adopted communication strategy along the FSO D-R links. Namely, these schemes will be referred to as the all-active and selective schemes. For all-active relaying, the information message is first transmitted from D (that now plays the role of the transmitting node) to all relays. The power will be evenly among all N FSO links and this scheme can be implemented in the absence of CSI. In the second RF hop, only one relay will retransmit its decoded version of the message to S (that will now play the role of the receiving node). Transmissions are restricted to only one relay in order to avoid interference along the RF communication links. While distributed space-time coding techniques can be applied along the RF hop, this selection scheme is appealing because of its simplicity and easy synchronization.

On the other hand, in the case of selective relaying, communications take place along the best end-to-end path. This path is defined as the one that results in the minimum BER for a given realization of the N RF channels and N FSO channels. This scheme necessitates acquiring full knowledge about the channel states (as well as the noise variances) for the sake of computing the error probabilities of the N available parallel end-to-end links.

For the sake of notational simplicity, we denote the conditional BER along the n-th FSO link by $Q_n(p_n)$ where, as in (7), p_n stands for the fraction of the optical power that is allocated to the n-th link. Defining X_1 (resp. X_2) as the Poisson rv whose parameter is given by $\mathrm{E}[X_n^{(\text{on})}]$ (resp. $\mathrm{E}[X_n^{(\text{off})}]$) in (7), then $P_n = \Pr(X_2 > X_1) + \frac{1}{2}\Pr(X_2 = X_1)$

$$P_{e|\mathcal{H},\mathcal{I}}^{(\text{SS-NCSI})} = \sum_{\mathcal{S}\subset\{1,\ldots,N\}} \prod_{n\in\mathcal{S}} \left(1 - Q\left(\sqrt{\frac{2k_nE_b}{N_0}}h_n\right)\right) \prod_{n'\in\overline{\mathcal{S}}} Q\left(\sqrt{\frac{2k_{n'}E_b}{N_0}}h_{n'}\right)$$
$$\left[\sum_{k=0}^{+\infty} e^{-N\lambda_b}\frac{(N\lambda_b)^k}{k!}\sum_{j=0}^{k-1} e^{-\left(\left(\frac{1}{N}\sum_{n\in\mathcal{S}} g_nI_n\right)\lambda_s+N\lambda_b\right)}\frac{\left(\left(\frac{1}{N}\sum_{n\in\mathcal{S}} g_nI_n\right)\lambda_s+N\lambda_b\right)^j}{j!}\right.$$
$$\left.+\frac{1}{2}\sum_{k=0}^{+\infty} e^{-N\lambda_b}\frac{(N\lambda_b)^k}{k!}e^{-\left(\left(\frac{1}{N}\sum_{n\in\mathcal{S}} g_nI_n\right)\lambda_s+N\lambda_b\right)}\frac{\left(\left(\frac{1}{N}\sum_{n\in\mathcal{S}} g_nI_n\right)\lambda_s+N\lambda_b\right)^k}{k!}\right] \quad (15)$$

$$P_{e|\mathcal{H},\mathcal{I}}^{(\text{SS-CSI})} = \sum_{\mathcal{S}\subset\{1,\ldots,N\}} \prod_{n\in\mathcal{S}} \left(1 - Q\left(\sqrt{\frac{2k_nE_b}{N_0}}h_n\right)\right) \prod_{n'\in\overline{\mathcal{S}}} Q\left(\sqrt{\frac{2k_{n'}E_b}{N_0}}h_{n'}\right)$$
$$\left[\sum_{k=0}^{+\infty} e^{-N\lambda_b}\frac{(N\lambda_b)^k}{k!}\sum_{j=0}^{k-1} e^{-\left(\max_{n\in\mathcal{S}}\{g_nI_n\}\lambda_s+N\lambda_b\right)}\frac{\left(\max_{n\in\mathcal{S}}\{g_nI_n\}\lambda_s+N\lambda_b\right)^j}{j!}\right.$$
$$\left.+\frac{1}{2}\sum_{k=0}^{+\infty} e^{-N\lambda_b}\frac{(N\lambda_b)^k}{k!}e^{-\left(\max_{n\in\mathcal{S}}\{g_nI_n\}\lambda_s+N\lambda_b\right)}\frac{\left(\max_{n\in\mathcal{S}}\{g_nI_n\}\lambda_s+N\lambda_b\right)^k}{k!}\right] \quad (18)$$

that can be developed as:

$$Q_n(p_n) = \sum_{k=0}^{+\infty} e^{-\lambda_b}\frac{\lambda_b^k}{k!}\sum_{j=0}^{k-1} e^{-(p_ng_nI_n\lambda_s+\lambda_b)}\frac{(p_ng_nI_n\lambda_s+\lambda_b)^j}{j!}$$
$$+\frac{1}{2}\sum_{k=0}^{+\infty} e^{-\lambda_b}\frac{\lambda_b^k}{k!}e^{-(p_ng_nI_n\lambda_s+\lambda_b)}\frac{(p_ng_nI_n\lambda_s+\lambda_b)^k}{k!} \quad (23)$$

1) All-Active Relaying: Denoting by $\mathcal{S}$ the set of relays that have successfully decoded the message and considering all possible subsets of $\{1,\ldots,N\}$ results in the following expression of the conditional BER:

$$P_{e|\mathcal{H},\mathcal{I}}^{(\text{Act.})} = \sum_{\mathcal{S}\subset\{1,\ldots,N\}} \prod_{n\in\mathcal{S}} \left(1 - Q_n\left(\frac{1}{N}\right)\right) \prod_{n'\in\overline{\mathcal{S}}} Q_{n'}\left(\frac{1}{N}\right)$$
$$\left[Q\left(\sqrt{\frac{2E_b\max_{n\in\mathcal{S}}\{k_nh_n^2\}}{N_0}}\right)\right] \quad (24)$$

where the last term (corresponding to the error probability along the strongest RF link) follows directly from (1). Evidently, the selection needs to be carried out among the relays that have successfully decoded the message. Terms of the form $Q_n(p_n)$ are defined in (23) when $p_n = \frac{1}{N}$ for $n = 1,\ldots,N$ since the optical power is evenly split among the N FSO links in the absence of CSI.

2) Selective Relaying: Assume that the n-th end-to-end path D-R$_n$-S was selected. An error will occur along this path either if an erroneous decision was made along the first FSO hop or if an erroneous decision was made along the second RF hop (note that a double error will result in a correct decision since the modulation schemes along the FSO and RF links are both binary). Consequently, the conditional error probability

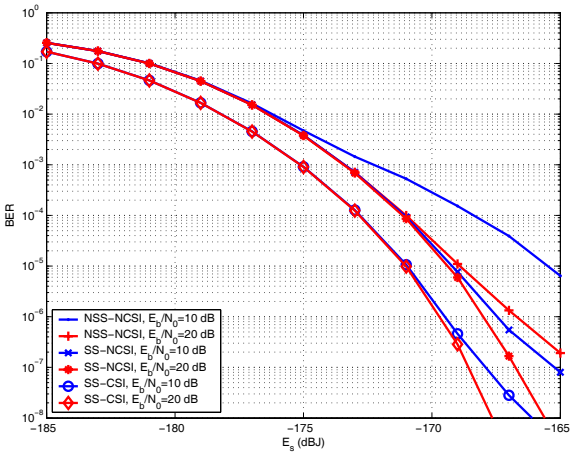

Fig. 2. Performance along the up-link with 3 relays.

of the selective scheme can be written as:

$$P_{e|\mathcal{H},\mathcal{I}}^{(\text{Sel.})} = \min_{n=1,\ldots,N}\left\{Q_n(1)\left(1 - Q\left(\sqrt{\frac{2k_nE_b}{N_0}}h_n\right)\right)\right.$$
$$\left.+\left(1-Q_n(1)\right)Q\left(\sqrt{\frac{2k_nE_b}{N_0}}h_n\right)\right\} \quad (25)$$

where p_n was set to 1 in (23) since the total optical power will be allocated to a single FSO link.

As in the case of the up-link, the average BERs can be determined by numerically integrating (24) and (25) using the pdf's of the RF and FSO path gains in (2) and (4).

IV. Numerical Results

In what follows, the operating wavelength and the refractive index structure constant are set to $\lambda = 1550$ nm and $C_n^2 = 1.7\times10^{-14}$ m$^{-2/3}$, respectively. In all considered scenarios,

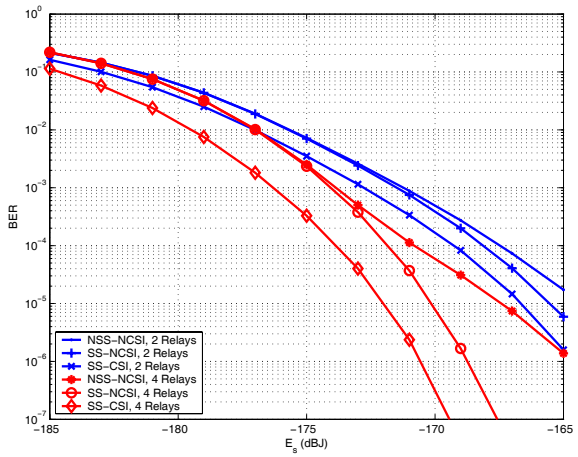

Fig. 3. Performance along the up-link with 2 and 4 relays.

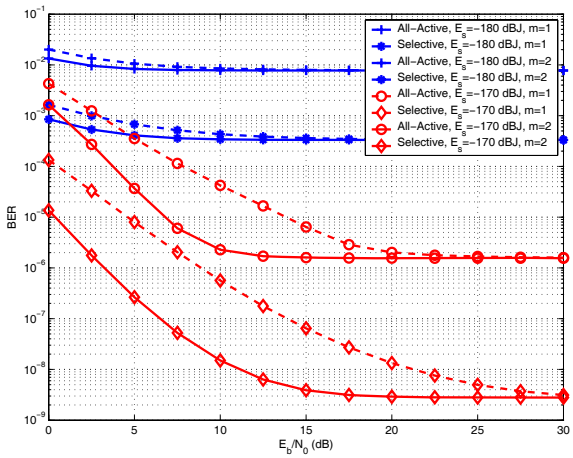

Fig. 4. Performance along the down-link with 3 relays.

the distance between S and D is assumed to be 3 km. We also fix $\Omega_n = 1$ for $n = 1, \ldots, N$ in (2).

Fig. 2 shows the performance along the up-link with three relays. The level of the optical background noise is determined from $\frac{P_b T_b}{2} = -190$ dBJ. The relays are placed at distances of 1.25 km, 1.5 km and 2 km from S and at distances of 2.5 km, 1.5 km and 1.75 km from D, respectively. The shape parameters of the Nakagami rv's are selected as $m_1 = 2.5$, $m_2 = 2$ and $m_3 = 1.5$ where shorter S-R distances are associated with larger values of m. Finally, the SNRs along the RF links are fixed to either 10 dB or 20 dB while the BERs are plotted as a function of E_s defined in (8). As expected, the SS-CSI and NSS-NCSI schemes result in the best and worst BER performances, respectively. Results also highlight that the gap between the NSS-NCSI scheme, on one hand, and the SS-NCSI and SS-CSI schemes, on the other hand, decreases as the SNR along the RF links increases since, in this case, the relays correctly decode the received message with high probability. Finally, at a BER of 10^{-4}, the SS-CSI scheme outperforms the SS-NCSI scheme by 2 dB.

Fig. 3 shows the performance along the up-link with two and four relays. A symmetrical network is considered where all relays are at distances of 1.5 km and 2.5 from S and D, respectively. We also fix $\frac{P_b T_b}{2} = -195$ dBJ, $\frac{E_b}{N_0} = 15$ dB and $m = 1.5$ for all relays. Results highlight the enhanced performance levels and diversity orders that follow from increasing the number of relays. For the SS-CSI scheme, the performance gain is in the order of 4.5 dB at a BER of 10^{-4}.

Fig. 4 shows the performance along the down-link with three relays. We fix $(d_{0,1}, d_{0,2}, d_{0,3}) = (1, 1.5, 2)$ km and $(d_{1,4}, d_{2,4}, d_{3,4}) = (2.5, 2, 1.5)$ km with $\frac{P_b T_b}{2} = -195$ dBJ. We fix E_s to either -180 dBJ or -170 dBJ and we plot the results as a function of the RF SNR $\frac{E_b}{N_0}$. Results highlight the presence of error floors where the performance is dominated by the quality of the FSO links. As expected, selective relaying results in higher performance gains especially for larger values of E_s. Results also highlight the impact of m on the performance especially for small values of the RF SNR.

V. Conclusion

We considered the problem of mixed RF/FSO relaying in the up-link and the down-link. In the first case, three protocols were analyzed based on the performed symbol selectivity and channel estimation while in the second case all-active relaying was compared with selective relying. The presented analysis highlighted the strengths and limitations of these protocols and showed distinct behaviors in the up-link and down-link.

References

[1] A. Akbulut, H. G. Ilk, and F. Ari, "Design, availability and reliability analysis on an experimental outdoor FSO/RF communication system," in *Transparent Optical Networks, 2005, Proceedings of 7th IEEE International Conference*, vol. 1, 2005, pp. 403–406.

[2] M. Usman, H.-C. Yang, and M.-S. Alouini, "Practical switching-based hybrid FSO/RF transmission and its performance analysis," *IEEE Photonics Journal*, vol. 6, no. 5, pp. 1–13, Oct. 2014.

[3] W. Zhang, S. Hranilovic, and C. Shi, "Soft-switching hybrid FSO/RF links using short-length raptor codes: design and implementation," *IEEE J. Select. Areas Commun.*, vol. 27, no. 9, pp. 1698–1708, Dec. 2009.

[4] A. AbdulHussein, A. Oka, T. T. Nguyen, and L. Lampe, "Rateless coding for hybrid free-space optical and radio-frequency communication," *IEEE Trans. Wireless Commun.*, vol. 9, no. 3, pp. 907–913, Mar. 2010.

[5] E. Lee, J. Park, D. Han, and G. Yoon, "Performance analysis of the asymmetric dual-hop relay transmission with mixed RF/FSO links," *IEEE Photon. Technol. Lett.*, vol. 23, no. 21, pp. 1642–1644, Nov. 2011.

[6] N. I. Miridakis, M. Matthaiou, and G. K. Karagiannidis, "Multiuser relaying over mixed RF/FSO links," *IEEE Trans. Commun.*, vol. 62, no. 5, pp. 1634–1645, May 2014.

[7] V. Jamali, D. S. Michalopoulos, M. Uysal, and R. Schober, "Link allocation for multiuser systems with hybrid RF/FSO backhaul: Delay-limited and delay-tolerant designs," *IEEE Trans. Wireless Commun.*, vol. 15, no. 5, pp. 3281–3295, May 2016.

[8] M. I. Petkovic, A. M. Cvetkovic, G. T. Djordjevic, and G. K. Karagiannidis, "Partial relay selection with outdated channel state estimation in mixed RF/FSO systems," *J. Lightwave Technol.*, vol. 33, no. 13, pp. 2860–2867, July 2015.

[9] E. Zedini, H. Soury, and M.-S. Alouini, "On the performance analysis of dual-hop mixed FSO/RF systems," *IEEE Trans. Wireless Commun.*, vol. 15, no. 5, pp. 3679–3689, May 2016.

[10] M. Safari and M. Uysal, "Relay-assisted free-space optical communication," *IEEE Trans. Wireless Commun.*, vol. 7, no. 12, pp. 5441 – 5449, Dec. 2008.

[11] C. Abou-Rjeily, "Performance analysis of selective relaying in cooperative free-space optical systems," *J. Lightwave Technol.*, vol. 31, no. 18, pp. 2965–2973, Sep. 2013.